

# Catalysis Science & Technology

Accepted Manuscript



This is an *Accepted Manuscript*, which has been through the Royal Society of Chemistry peer review process and has been accepted for publication.

*Accepted Manuscripts* are published online shortly after acceptance, before technical editing, formatting and proof reading. Using this free service, authors can make their results available to the community, in citable form, before we publish the edited article. We will replace this *Accepted Manuscript* with the edited and formatted *Advance Article* as soon as it is available.

You can find more information about *Accepted Manuscripts* in the [Information for Authors](#).

Please note that technical editing may introduce minor changes to the text and/or graphics, which may alter content. The journal's standard [Terms & Conditions](#) and the [Ethical guidelines](#) still apply. In no event shall the Royal Society of Chemistry be held responsible for any errors or omissions in this *Accepted Manuscript* or any consequences arising from the use of any information it contains.

# Ionic tagged DABCO grafted on magnetic nanoparticles: a water-compatible catalyst for aqueous aza-Michael addition of amines to $\alpha,\beta$ -unsaturated amides

Anguo Ying<sup>a\*</sup>, Shuo Liu<sup>b</sup>, Yuxiang Ni<sup>b</sup>, Fangli Qiu<sup>a</sup>, Songlin Xu<sup>b\*</sup>, Wenyuan Tang<sup>a</sup>

(<sup>a</sup> *School of Pharmaceutical and Chemical Engineering, Taizhou University, Taizhou 318000*)

(<sup>b</sup> *School of Chemical Engineering and Technology, Tianjin University, Tianjin 300072*)

**Abstract** Ionic tagged 1,4-Diazabicyclo[2.2.2]octane (DABCO) grafted on magnetic nanoparticles (MNPs) was prepared and characterized by X-ray diffraction (XRD), transmission electron microscopy (TEM), Fourier transform infrared spectroscopy (FT-IR), vibrating sample magnetometer (VSM) and thermal gravimetric analysis (TGA). The resulting magnetic solid supported DABCO catalyst with ionic moiety was efficient for aza-Michael addition of aliphatic amines to various  $\alpha,\beta$ -unsaturated amides in water at room temperature, affording the desired products in good to excellent yields. Gratifying, the catalyst could be readily recovered by an external magnet and reused for ten times without significant loss of activity.

**Keywords** Magnetic nanoparticles, immobilization, aza-Michael addition, unsaturated amide, recyclability.

## Introduction

$\beta$ -Amino amides as well as their derivatives are found in many natural and pharmaceutical compounds that express potential biological activities[1]. For example, dual acetylcholinesterase (AChE) inhibitor **1** have been approved by FDA for the treatment of Alzheimer's disease (AD)[2].

---

\* Corresponding authors. Tel/fax: +86 576 88660359.

E-mail address: yinganguo@163.com or [agyng@tzc.edu.cn](mailto:agyng@tzc.edu.cn) (A. Ying), [slxu@tju.edu.cn](mailto:slxu@tju.edu.cn) (S. Xu).

Electronic supplementary information (ESI) available: detailed NMR spectra of IS and unknown addition products.

The ethyl sulfide **2** with an  $IC_{50}=100\text{nM}$  against MetAP2 show growth inhibition property against HUVECs[1b]. Triazolopiperazine **3** is a DPP-4 inhibitor for the treatment of the type 2 diabetes[1e].  $\alpha$ -Hydroxy- $\beta$ -amino amides **4** is a key intermediate for the preparation of P1- $\alpha$ -ketoamides, which demonstrate potent inhibition of aminopeptidases and prolyl endopeptidases[3].

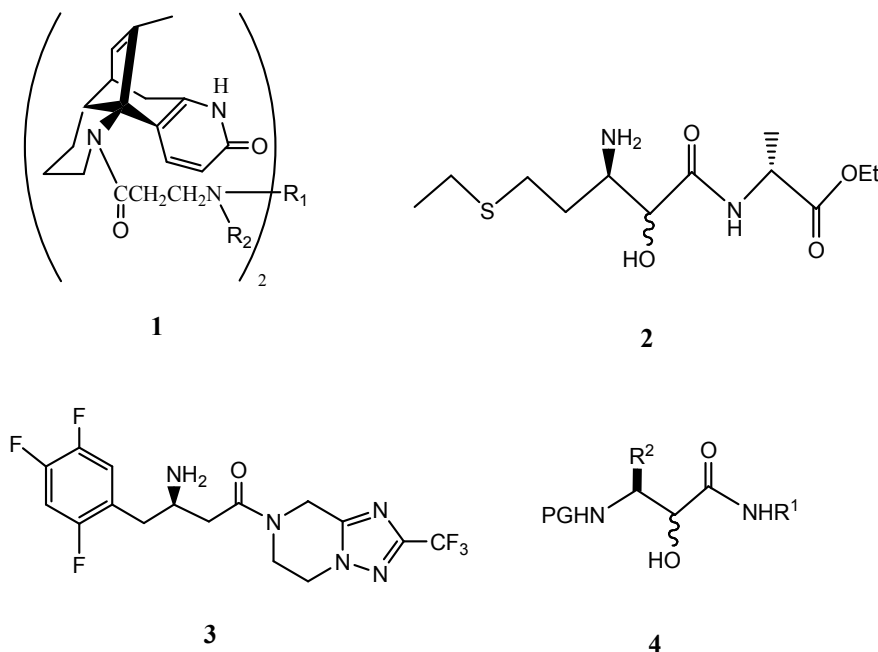


**Fig.1** Representative examples of biologically active products containing  $\beta$ -amino amide moiety

In view of excellent pharmaceutical activities of  $\beta$ -amino amides based compounds, much attention has been attracted to the construction and synthesis of these analogues[3,4]. As an atom-economic, simply and highly efficient synthetic method, Michael addition has been widely utilized in organic transformations. Accordingly, the conjugated addition of amines to  $\alpha,\beta$ -unsaturated amides has been frequently exploited as fascinating protocol to prepare  $\beta$ -amino amides. Several procedures have been reported to construct  $\beta$ -amino amides over the past few years using a variety of catalysts such as boric acid[5a], bromodimethylsulfonium bromide[5b],  $\text{KF}/\text{Al}_2\text{O}_3$ [5c],  $\text{LiClO}_4$ [5d],  $\text{Cu}(\text{acac})_2$  immobilized in ionic liquids[5e], polymer supported

gadolinium triflate[5f], phosphate impregnated titania[5g], ionic liquids[5h,5i] and silica gel[5j]. Very recently, Cooks presented a novel C-N bond formation reaction occurring in thin films deposited on ambient surfaces, providing an alternative method for the rapid synthesis of reaction product on a small scale[6]. Despite the remarkable success of the protocols mentioned above, however, most of them suffered from one or some drawbacks, for example, substrate-selective and air-sensitive for some catalysts, large amount catalyst loading, utilization of heavy metal salts coupled with volatile and harmful organic solvents, as well as tedious work-up and difficult recovery of catalyst. Thus, the development of a novel, efficient catalyst for aza-conjugate reaction of amines with  $\alpha,\beta$ -unsaturated amides is highly desirable.

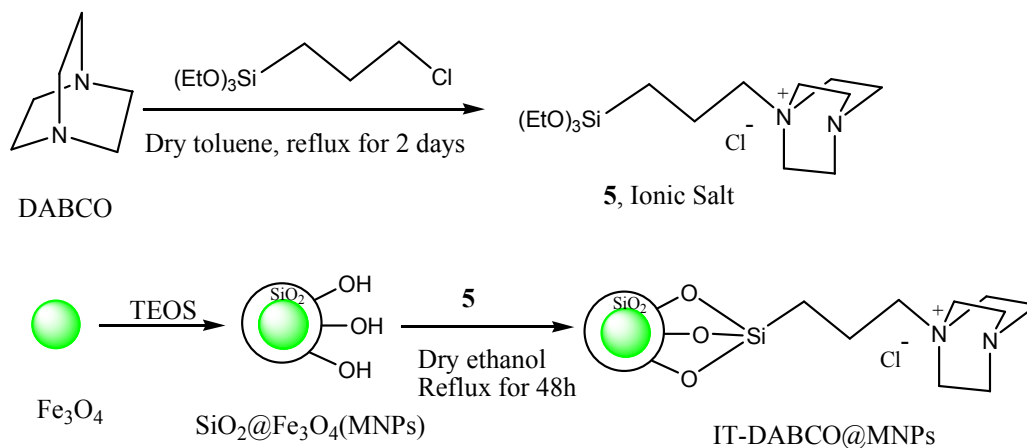
Magnetic nanoparticles (MNPs) as catalyst supports have been attracting more and more attention because they are not only readily dispersed in reaction solution with intrinsically high surface area rendering the efficient accessibility of substrates to the surface bound to the active catalytic sites, but also they are super-paramagnetic and can be easily recovered from the reaction mixture using an external magnet[7]. Thus, a lot of MNPs supported catalysts with excellent catalytic activities, have been developed and applied in versatile organic synthesis, including coupling reactions[8a-c], Ritter reaction[8d], cyanosilylation of carbonyl compounds[8e], Friedlander reaction[8f], reduction of  $\alpha,\beta$ -epoxy ketones[8g], and some enantioselective reactions[8h-j]. Very recently, to combine the magnetic nano-support features and unique properties of ionic moiety which usually facilitates accessibility of reactant to active site on the surface of the catalysts, as well as stabilizes the formed intermediates during reaction process[9], MNPs supported acidic[10] and chiral catalysts[11] with ionic tags were successfully prepared and exploited to promote the one-pot synthesis of benzoxanthenes and the direct asymmetric aldol

reaction, respectively. Herein, we present MNPs supported 1,4-Diazabicyclo[2.2.2]octane (DABCO) with ionic tag and its application as catalyst for aza-Michael addition of amines to  $\alpha,\beta$ -unsaturated amides.

## Results and discussion

### Preparation and characterization of the catalyst

The magnetic nanoparticle supported DABCO with ionic tag (IT-DABCO@MNPs) was prepared following the procedure depicted in Scheme 1. The first step was to prepare  $\text{Fe}_3\text{O}_4$  nanoparticles, starting from commercially available ferric chloride hexahydrate and ferrous chloride tetrahydrate[12]. To prevent the aggregation of the  $\text{Fe}_3\text{O}_4$  particles and provide numerous surface Si-OH groups for further modifications, silica as a protecting shell was utilized to coat the naked particles to form a core-shell structure ( $\text{SiO}_2@\text{Fe}_3\text{O}_4$ ) by a chemical co-precipitating method according with the reported literature 13. Ionic salt **5** was synthesized by quaternization of DABCO with triethoxy-3-(chloropropyl)-silane in dry toluene refluxing for 48 hours. Then MNPs ( $\text{SiO}_2@\text{Fe}_3\text{O}_4$ ) with abundant surface hydroxyl groups were selected as carriers to graft the ionic salt **5** to give the desired catalyst IT-DABCO@MNPs as grey solid.



### Scheme 1 Synthesis of ionic tagged DABCO grafted on MNPs

The XRD patterns of carrier  $\text{SiO}_2@\text{Fe}_3\text{O}_4$  (MNPs) and catalyst IT-DABCO@MNPs show the typical peaks at  $30.07^\circ$ ,  $35.52^\circ$ ,  $43.12^\circ$ ,  $53.36^\circ$ ,  $57.19^\circ$ ,  $62.79^\circ$  with the corresponding reflections of (220), (311), (400), (422), (511), (440) crystal planes as indicated in Fig. 2. Comparing the XRD pattern of MNPs and catalyst IT-DABCO@MNPs, immobilization of IS 5 on the surface of the MNPs did not significantly affect the structure of  $\text{Fe}_3\text{O}_4$  nanoparticles and they both match well with the data for standard  $\text{Fe}_3\text{O}_4$  sample[14]. A broad peak in the XRD pattern of IT-DABCO@MNPs at  $2\theta=22-26^\circ$  is the characteristics of amorphous silica shell of the silica coated nanoparticles ( $\text{SiO}_2@\text{Fe}_3\text{O}_4$ ) [15].

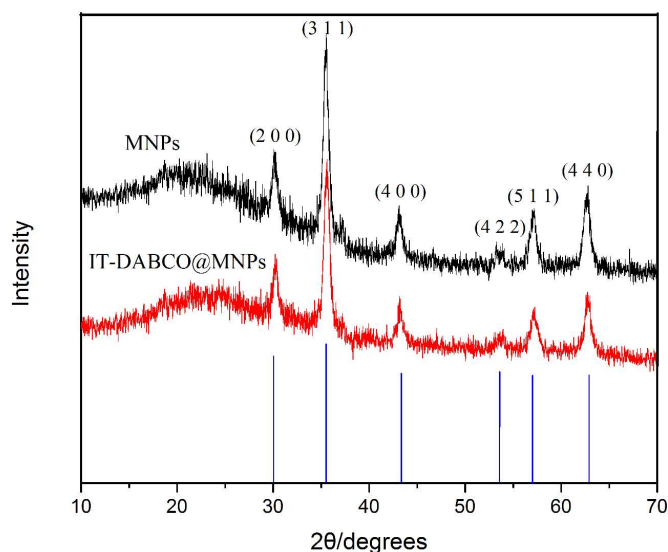


**Fig.2** Powder X-ray diffraction patterns of MNPs and IT-DABCO@MNPs

The transmission electron microscope (TEM) images of bare  $\text{Fe}_3\text{O}_4$ , silica coated nanoparticles (MNPs) and IT-DABCO@MNPs were confirmed that three samples have uniform-sized magnetic nanoparticles with almost spherical morphology. The silica shell on the bare  $\text{Fe}_3\text{O}_4$  is 3-5 nm thick(Fig.3a). For comparison with  $\text{SiO}_2@\text{Fe}_3\text{O}_4$  (Fig.3a), the grey shell in Fig.3b and Fig.3c

exhibits thickness of 5-15 nm, demonstrating the successful immobilization of ionic salt **5** on the nanoparticles. The loading of IS **5** per g was determined to be 1.41 mmol g<sup>-1</sup> by elemental analysis of nitrogen.

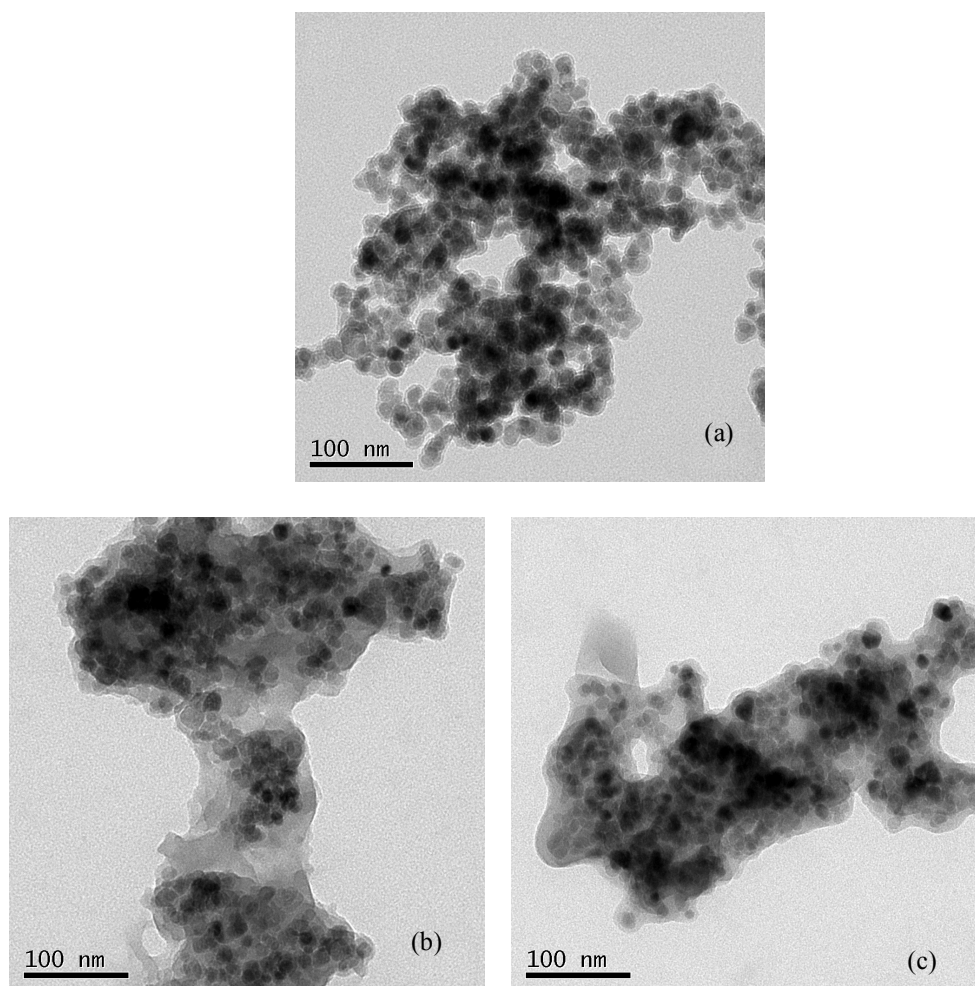


**Fig.3** Transmission electron microscope (TEM) images of SiO<sub>2</sub>@Fe<sub>3</sub>O<sub>4</sub>(a), fresh IT-DABCO@MNPs (b), IT-DABCO@MNPs after ten times reused(c).

Successful functionalization of the MNPs with DABCO based salt **5** was further confirmed by Fourier transform infrared spectroscopy (FT-IR) analysis. The blank MNPs, ionic salt **5** and IT-DABCO@MNPs were intensively investigated (Fig.4). As shown in Fig.4, the spectrum for the MNPs along exhibits a peak at 575 cm<sup>-1</sup> and stretching vibration at 1080 cm<sup>-1</sup> which are attributed

to the Fe-O vibration and Si-O-Si modes of the silica shell, respectively. The two characteristic vibrations can also be observed in the spectrum of immobilized catalyst IT-DABCO@MNPs, proving that surface modification on the particles has not bring change regarding the properties of magnetic core at all. Both IS **5** and IT-DABCO@MNPs shows typical peaks at  $1472\text{ cm}^{-1}$ ,  $2887\text{ cm}^{-1}$ ,  $2972\text{ cm}^{-1}$ , which can be assigned to the alkyl chain stretching and deformation vibrations[10]. The presence of C-N bond at the DABCO structure was evident from characteristic band at  $1210\text{ cm}^{-1}$ .

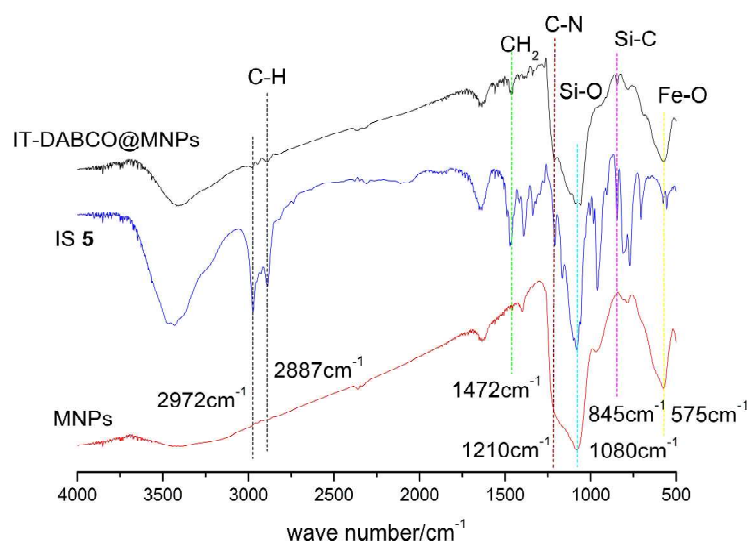


**Fig.4** FT-IR spectra of IT-DABCO@MNPs, ionic salt **5** and  $\text{SiO}_2@\text{Fe}_3\text{O}_4$ .

The magnetism of samples was characterized by vibrating sample magnetometer (VSM) at room temperature. As shown in Fig.5, the two examples both present excellent paramagnetism and can be completely saturated at high fields of up to 2.0 T. When the IS **5** was grafted on the surface of the carrier MNPs ( $\text{SiO}_2@\text{Fe}_3\text{O}_4$ ), the saturated magnetism was decreased from 59.2 to 34.6  $\text{emu g}^{-1}$ . The efficient magnetization of catalyst IT-DABCO@MNPs can also be verified by simple attraction with external magnetic forces during the reaction workup process (Fig.8b).

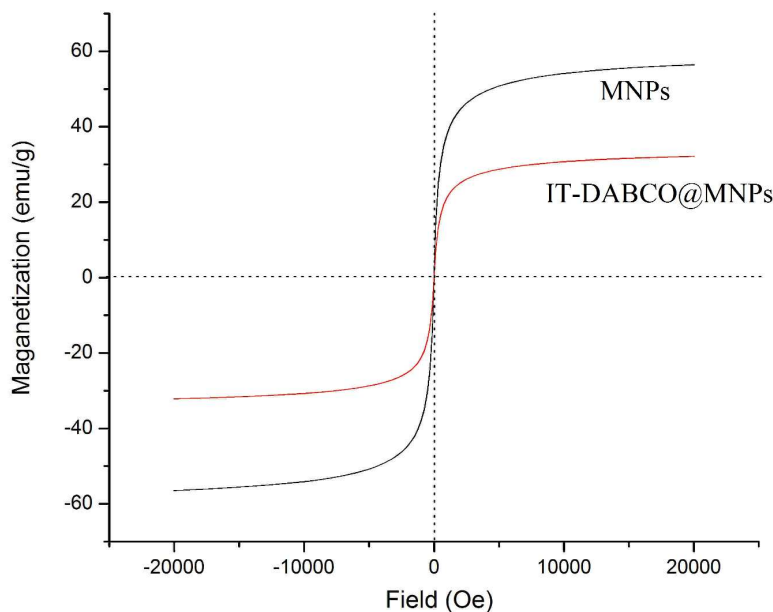


**Fig.5** Magnetic curves of MNPs and IT-DABCO@MNPs

The stability of the supported catalyst IT-DABCO@MNPs was investigated by the thermogravimetric (TG) analysis, which is also one indication of bond formation between MNPs and catalyst. As shown in Fig.6, an initial loss from room temperature to 238 °C was detected due to the removal of surface absorbed water and structural water within amorphous SiO<sub>2</sub>[16]. The second weigh loss at 239-400 °C was assigned to complete cleavage of DABCO moiety grafted on the shell around the nanoparticles and the amount of the organic DABCO was approximately 16.5 % against the total solid catalyst. The last weigh loss was at the temperature range of from 401 °C to 540 °C, probably due to the decomposition of trialkoxysilane moiety[11,17]. The peak in DTG curve demonstrates that the most fastest weigh loss occurred between 239 °C and 323 °C. Thus, the rational and safe temperature for its catalytic performance is around or below 239 °C.

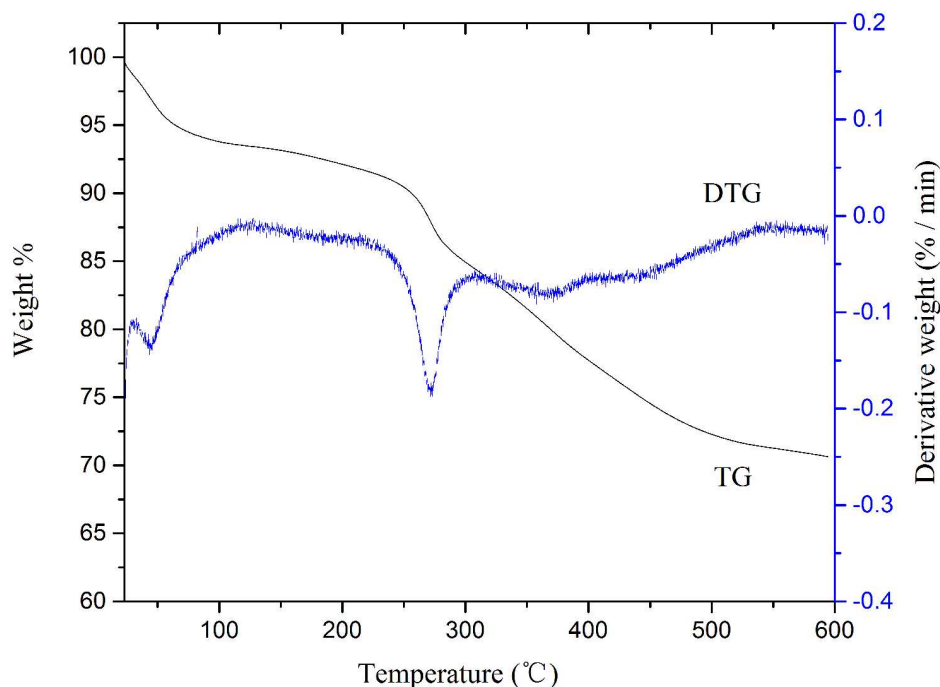


**Fig.6** Thermogravimetric (TG) and different thermogravimetric (DTG) analysis of catalyst

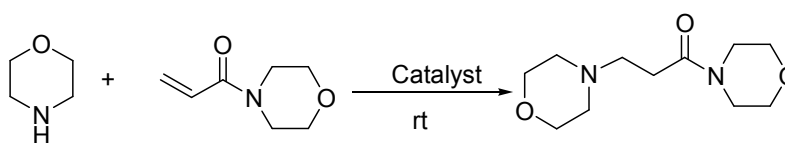
IT-DABCO@MNPs

#### **IT-DABCO@MNPs catalyzed aza-Michael addition of amines to $\alpha,\beta$ -unsaturated amides**

We tested the catalytic activity of supported catalyst IT-DABCO@MNPs using aza-Michael addition of morpholine to 4-acryloylmorpholine as model reaction. In an effort to establish a better catalytic system, the effects of solvent, catalyst, amount of catalyst on aza-Michael addition were thoroughly evaluated on the model reaction at room temperature. As shown in Table 1, solvent is a crucial factor for the reaction results in terms of reaction rate and yield. Protic solvents including methanol and water gave good reaction yields within 3 hours while aprotic solvents gave significantly lower yields (Table 1, entries 1-4). From both viewpoint of environmentally benign green chemistry and reaction results, water was finally selected as the suitable medium for further

examinations. Then, a series of catalysts were exploited to promote the reaction of morpholine and 4-acryloylmorpholine (Table 1, entries 4-7). Organic base triethylamine was found to be effective for the reaction affording the desired product in 65 % yield in 4 hours. Very interestingly, ionic tagged DABCO grafted on MNPs (IT-DABCO@MNPs) show much better catalytic activity than its corresponding organic base DABCO (Table 1, entries 4 and 5). When the reaction was catalyzed by MNPs or in absence of any catalyst, almost no reaction product was detected (Table 1, entries 6 and 7). With the increasing amount of the catalyst from 1.0 mol % (Table 1, entries 4 and 11-12), the desired product yield does not further increase while reducing the amount of the catalyst leads to the obviously decreased yield (Table 1, entries 4 and 9-10). Therefore, 1.0 mol % of IT-DABCO@MNPs with water as solvent was enough to push the reaction to completion.

**Table 1** Conjugated addition of morpholine (5 mmol) to 4-acryloylmorpholine (6 mmol) under different reaction conditions



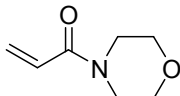
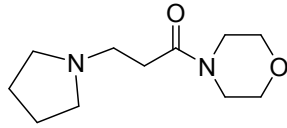
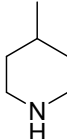
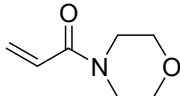
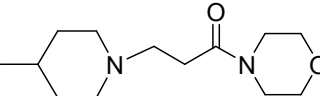
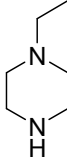
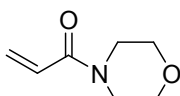
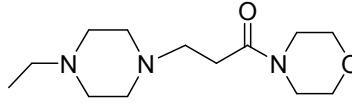
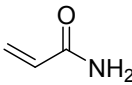
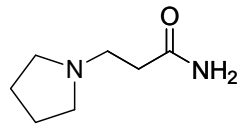
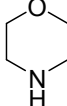
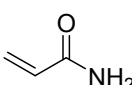
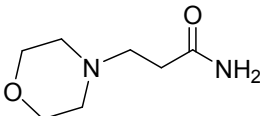
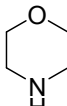
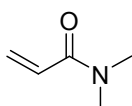
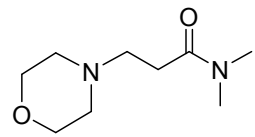
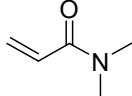
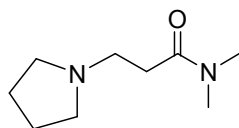
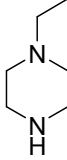
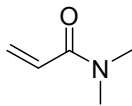
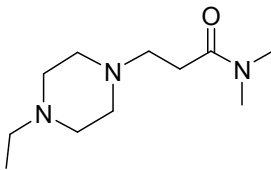
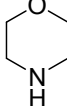
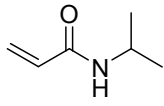
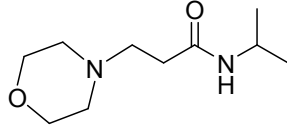
Entry	Catalyst (mol %)	Solvent <sup>b</sup>	Time (h)	Yield (%) <sup>a</sup>
1	IT-DABCO@MNPs (1.0)	CH <sub>2</sub> Cl <sub>2</sub>	5	13
2	IT-DABCO@MNPs (1.0)	Toluene	5	8
3	IT-DABCO@MNPs (1.0)	methanol	3	69
4	IT-DABCO@MNPs (1.0)	Water	2	84
5	DABCO (2.0)	Water	4	76
6	Et <sub>3</sub> N (2.0)	Water	4	65

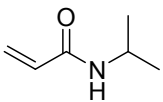
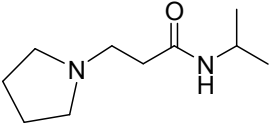
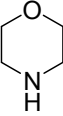
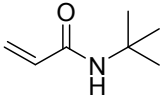
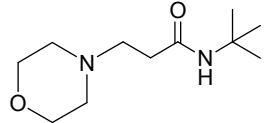
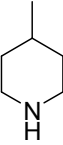
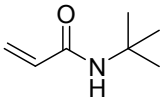
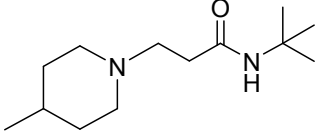
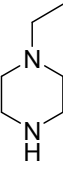
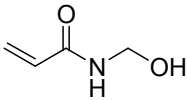
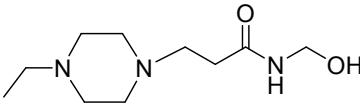
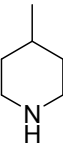
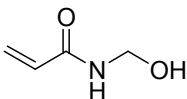
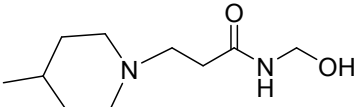
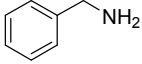
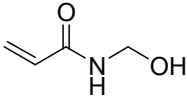
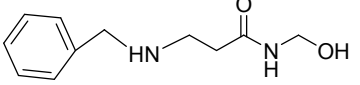
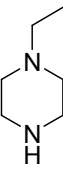
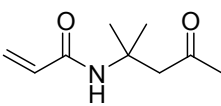
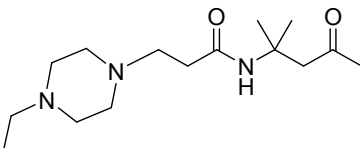
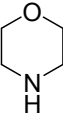
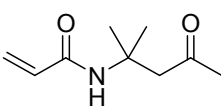
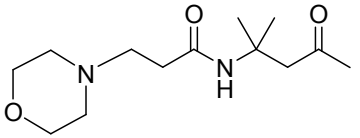
7	SiO <sub>2</sub> @Fe <sub>3</sub> O <sub>4</sub> (MNPs) (150 mg)	Water	8	Trace
8	-	Water	24	NR <sup>c</sup>
9	IT-DABCO@MNPs (0.5)	Water	3	65
10	IT-DABCO@MNPs (0.1)	Water	3	38
11	IT-DABCO@MNPs (1.5)	Water	2	84
12	IT-DABCO@MNPs(3.0)	Water	2	85

<sup>a</sup> Isolated yield based on morpholine. <sup>b</sup> The volume of solvent is 10 mL. <sup>c</sup> NR: no reaction.

With the optimal reaction conditions in hand as well as to study the generality of this procedure, we then proceeded to explore a wide range of aliphatic amines and  $\alpha,\beta$ -unsaturated amides (Table 2). As shown in Table 2, the reaction of various aliphatic amines and *N*-substituted acrylamides underwent smoothly to yield the desired adducts in good to excellent yields. Pyrrolidine, *N*-methyl-piperidine and *N*-ethyl-piperazine were efficient donors to react with 4-acryloylmorpholine to generate the conjugated products in the yields of 75 %-89 % (Table 2, entries 1-3). It has been observed that the reaction is greatly influenced by the steric hindrance. In other word, the larger the substituent on N position of the acrylamide is, the lower the reaction rate is (Table 2, entries 5,6,9,11). To our pleasure, *N*-hydroxymethyl acrylamide and diacetone acrylamide are also efficient Michael acceptors to give the corresponding products with reasonable yields (Table 2, entries 13-17). Finally, chem-selectivity of IT-DABCO@MNPs was examined in the reaction of 4-acryloylmorpholine and *N*-(2-hydroxyethyl)piperazine (Scheme 2). 85 % Yield of adduct formed by nitrogen nucleophile attack was obtained while no side product formed via oxygen nucleophile addition was detected, demonstrating the excellent chem-selectivity of IT-DABCO@MNPs.

**Table 2** aza-Michael reaction catalyzed by IT-DABCO@MNPs in water<sup>a</sup>

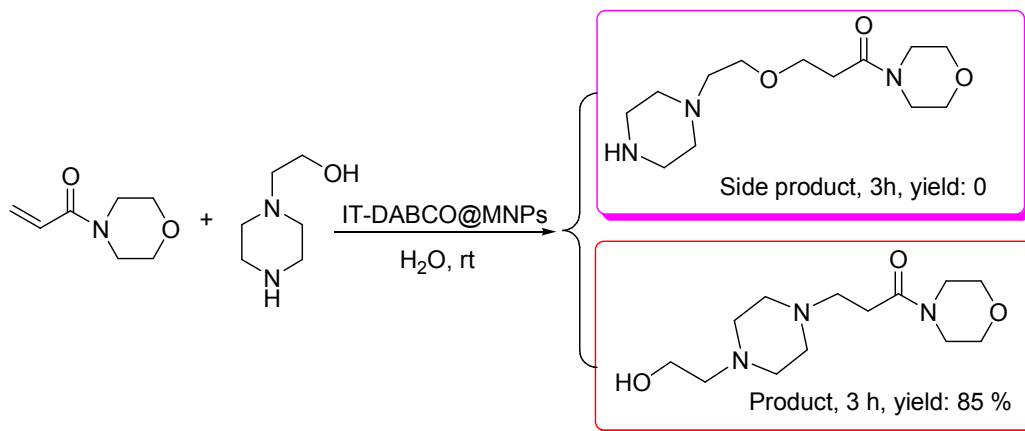
Entry	Amine	$\alpha,\beta$ -Unsaturated amide	Product	Time (h)	Yield (%) <sup>b</sup>	Ref.
1				2	89	18a
2				2	89	-
3				3	75	-
4				1	92	5j
5				1	87	5j
6				2	83	-
7				3	91	18b
8				1	88	-
9				3	75	-

10				3	93	-
11				3	70	18c
12				3	86	-
13				1	92	-
14				1	91	-
15				5	65	18c
16				2	91	-
17				5	70	-

<sup>a</sup> Reactions were carried out on 5.0 mmol scale of amine with 1.2 equiv of  $\alpha,\beta$ -unsaturated amide

in the presence of 1.0 % mol of IT-DABCO@MNPs in water (10 mL) at room temperature. <sup>b</sup>

Isolated yield based on amine.



**Scheme 2** Investigation of chem-selectivity of catalyst IT-DABCO@MNPs

A plausible mechanism for the aza-Michael reaction between amine and  $\alpha,\beta$ -unsaturated amide is depicted in Fig.7. The reaction proceeds *via* the initial formation of hydrogen bond (in state **B**) between catalyst **A** and amine, which is favorable to produce nitrogen anion (state **C**). Subsequently, the nucleophile reacts with unsaturated amide to give the final target product and release the catalyst IT-DABCO@MNPs. The catalyst IT-DABCO@MNPs (**A**) has two domains. One is the functional domain, in which nitrogen provides a hydrogen bond acceptor. The remained domain as well as OH group on the surface of the silica coated magnetic nanoparticles makes the catalyst compatible with water and being applied in environmental benign aqueous conditions. Moreover, the “ionic environment” present electrosteric activation to stabilize the transition-state [9b]. All of these novel features as well as high surface area of the MNPs-supported catalyst facilitate the reaction efficiently.



ethyl acetate to obtain crude product, followed by column flash chromatography for further purification. The recovered catalyst was washed with methanol, dried under vacuum and subjected to the next run.. For comparison, the reuse of free base DABCO was also tested in the same model reaction. The IT-DABCO@MNPs could be recycled up 10 times without any significant loss of activity while remarkably decrease in the yield was observed using DABCO as catalyst (Fig.9). The reason is that after the ten usage, the ionic tagged DABCO moiety has not degraded from the magnetic carrier, judging from the FT-IR spectra (Fig.10) and the TEM observation of the recovered catalyst (Fig.3c). Moreover, the loading of DABCO residue subjected ten recycle reaction is  $1.28 \text{ mmol g}^{-1}$ , slightly lower than that of fresh catalyst IT-DABCO@MNPs ( $1.41 \text{ mmol g}^{-1}$ ). On the contrary, DABCO was greatly washed away during the workup process of extraction, leading to its bad recyclability.

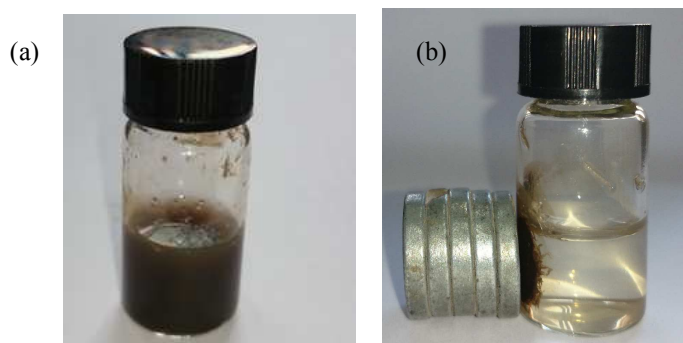


**Fig.8** Photographs of the dispersion of the catalyst IT-DABCO@MNPs in water (a) and the separation with an external magnet (b).

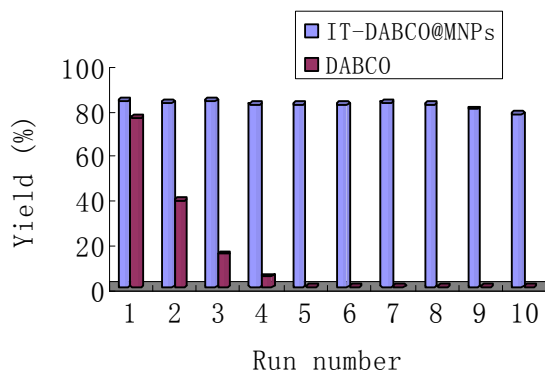


**Fig.9** Reuse of the catalyst IT-DABCO@MNPs (reaction time: 2h) and DABCO (reaction time: 4h) in the aqueous reaction of morpholine and 4-acryloylmorpholine.

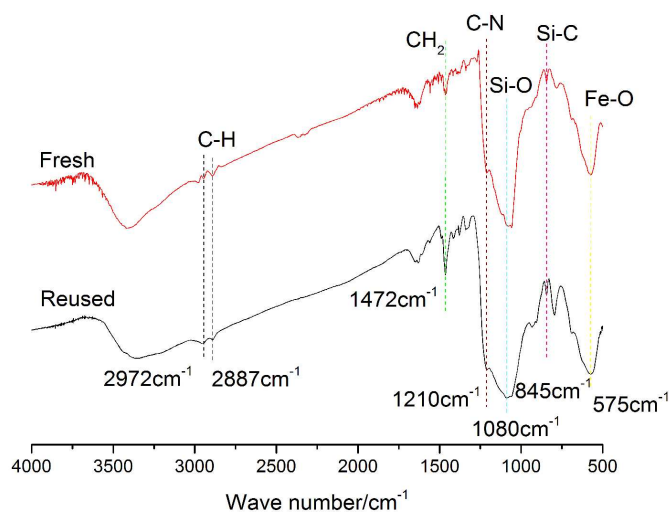


**Fig.10** FT-IR spectra of fresh catalyst IT-DABCO@MNPs and catalyst subjected to reused ten times.

## Conclusions

In conclusion, a magnetically recoverable DABCO catalyst with ionic tag (IT-DABCO@MNPs) was successfully prepared and was subsequently used in aqueous aza-Michael addition of various amines to a wide range of  $\alpha,\beta$ -unsaturated amides at room temperature with success. The presence

of the ionic tag or ionic environment in the supported catalyst make it water-compatible and effective for the type of reaction. In addition, the catalyst is reusable for ten cycles without any significant loss of its catalytic activity. Further applications of the catalyst to other organic transformations are undergoing in our laboratory.

## Experimental

### Materials and instruments

All chemical reagents were purchased without further purification. The reaction monitoring was accomplished by thin layer chromatography (TLC) on gel F254 plates. Powder X-ray diffraction data were obtained Cu K $\alpha$  radiation. Fourier transform infrared spectroscopy (FT-IR) were recorded on a spectrometer using KBr pellets. Transmission electron microscopy (TEM) was performed with a instrument operating at 40-100 kV. The magnetic measurements were carried out in a vibrating sample magnetometer (VSM) at room temperature.  $^1\text{H}$  and  $^{13}\text{C}$  NMR were recorded on a spectrometer at 400 MHz and 100 MHz in  $\text{CDCl}_3$ , respectively. Chemical shifts were reported in parts per million ( $\delta$ ), relative to the internal standard of tetramethylsilane (TMS).

### Preparation of silica coated magnetic nanoparticle-SiO<sub>2</sub>@ Fe<sub>3</sub>O<sub>4</sub> (MNPs)

Magnetic (Fe<sub>3</sub>O<sub>4</sub>) nanoparticles were prepared by the coprecipitation [12]. FeCl<sub>3</sub>·6H<sub>2</sub>O (8.1 g, 0.03 mmol) and FeCl<sub>2</sub>·4H<sub>2</sub>O (4.97 g, 0.025 mmol) were dissolved in distilled water (100 mL). The resulting transparent solution was heated at 85 °C with vigorous mechanically stirring under N<sub>2</sub> atmosphere for 1 h. The pH value was then adjusted to 9 using the concentrated aqueous ammonia (25 wt %). After the color of the bulk solution turned to black, the magnetic precipitates were separated and washed several times with deionized water until the pH value of the eluent

decreased to 7. The coating of a layer of silica on the surface of the naked  $\text{Fe}_3\text{O}_4$  was conducted through sol-gel method [13]. The naked  $\text{Fe}_3\text{O}_4$  (1.0 g) was dispersed in ethanol (200 mL) by ultrasonic irradiation. The concentrated  $\text{NH}_3\cdot\text{H}_2\text{O}$  (6 mL) and TEOS (2 mL) were successively added into the solution. With continuous stirring for 24 h at room temperature. The resulting MNPs was collected by an external magnet and washed three times with ethanol, followed by drying in vacuum.

#### **Synthesis of the catalyst IT-DABCO@MNPs**

To a solution of DABCO (5.6 g, 50 mmol) in dry toluene (50 mL), 3-chloropropyltriethoxysilane (12.0 mL, 50 mmol) was added and the mixture was refluxed for 48 h under nitrogen atmosphere. TLC showed the completion of the reaction. The reaction mixture was evaporated under reduced pressure, followed by dried under vacuum for 6 h to give intermediate ionic salt **5** as a white solid in 96 % yield.

The obtained MNPs powder (2 g) was dispersed in 30 mL toluene by sonication for 1 h., and then ionic salt **5** (0.5 g) was added to the mixture. After mechanical stirring in reflux under nitrogen atmosphere for 48 h, the suspended solid was separated by an external magnet and rinsed with ethanol for three times and then dried under vacuum for 8 h to afford the final catalyst as grey solid (2.28 g).

NMR data for ionic salt **5**

$^1\text{H}$  NMR (400MHz,  $\text{D}_2\text{O}$ ):  $\delta$  3.82-3.87(m, 3H), 3.55-3.61(m, 3H), 3.32-3.36(m, 6H), 3.19-3.23(m, 2H), 3.11-3.15(m, 6H), 1.76-1.85(m, 2H), 1.18(t, 4H), 1.12(t, 5H), 0.56-0.73(m, 2H);  $^{13}\text{C}$  NMR (100MHz,  $\text{D}_2\text{O}$ ):  $\delta$  66.4, 57.5, 52.2, 44.3, 16.9, 15.4.

**General procedure for the IT-DABCO@MNPs catalyzed ambient aza-Michael addition of**

**amines to  $\alpha,\beta$ -unsaturated amides in water**

A mixture of amine (5 mmol),  $\alpha,\beta$ -unsaturated amide (6 mmol), water (20 mL) and IT-DABCO@MNPs (35 mg) was stirred at room temperature. Upon the completion of the reaction (monitored by TLC), the catalyst, separated from the reaction solution by external magnet, washed with ethanol and ethyl acetate, followed by drying under vacuum, was reused for subsequent runs. The decanting solution was directly filtrated and the remained residue was extracted with ethyl acetate. The resulting crude product was purified by column chromatography using petroleum ether/ethyl acetate as the eluent. The products were characterized by  $^1\text{H}$  NMR,  $^{13}\text{C}$  NMR and elemental analysis.

NMR data for non-published products

3-(4-Methylpiperidin-1-yl)-1-morpholinopropan-1-one (Table 2, entry 2)

$^1\text{H}$  NMR (400 MHz,  $\text{CDCl}_3$ ) (ppm): 3.71(d, 1H,  $J=2.8\text{Hz}$ ), 3.65(d, 4H,  $J=3.6\text{Hz}$ ), 3.59(s, 3H), 3.47(s, 2H), 3.01(d, 2H,  $J=11.6\text{Hz}$ ), 2.83(t, 2H,  $J=7.6\text{Hz}$ ), 2.64(t, 2H,  $J=7.6\text{Hz}$ ), 2.15(t, 2H,  $J=7.6\text{Hz}$ ), 1.96(s, 1H), 1.65(d, 2H,  $J=12.8\text{Hz}$ ), 0.92(d, 3H,  $J=6.0\text{Hz}$ );  $^{13}\text{C}$  NMR (100 MHz,  $\text{CDCl}_3$ ) (ppm): 170.0, 72.5, 66.8, 66.6, 61.6, 53.7, 53.6, 45.9, 41.9, 33.2, 30.2, 30.0, 21.5. Anal. Calcd for  $\text{C}_{13}\text{H}_{24}\text{N}_2\text{O}_2$ : C, 64.97; H, 10.07; N, 11.66; O, 13.31. Found: C, 64.83; H, 10.23; N, 11.55; O, 13.39.

3-(4-Ethylpiperazin-1-yl)-1-morpholinopropan-1-one (Table 2, entry 3)

$^1\text{H}$  NMR (400 MHz,  $\text{CDCl}_3$ ) (ppm): 3.49-3.55(m, 6H), 3.36(s, 2H), 2.63(d, 2H,  $J=8.0\text{Hz}$ ), 2.33-2.46(m, 12H), 0.98(t, 3H,  $J=7.2\text{Hz}$ );  $^{13}\text{C}$  NMR (100 MHz,  $\text{CDCl}_3$ ) (ppm): 170.2, 66.7, 66.5, 53.8, 52.7, 52.2, 52.0, 45.9, 41.8, 30.4, 11.6. Anal. Calcd for  $\text{C}_{13}\text{H}_{25}\text{N}_3\text{O}_2$ : C, 61.15; H, 9.87; N, 16.46; O, 12.53. Found: C, 61.10; H, 9.91; N, 16.43; O, 12.56.

*N,N*-dimethyl-3-morpholinopropanamide (Table 2, entry 6)

$^1\text{H}$  NMR (400 MHz,  $\text{CDCl}_3$ ) (ppm): 3.68(t, 4H,  $J=4.8\text{Hz}$ ), 2.98(s, 3H), 2.91(s, 3H), 2.67-2.72(m, 2H), 2.51(d, 2H,  $J=8.0\text{Hz}$ ), 2.46-2.48(m, 4H);  $^{13}\text{C}$  NMR (100 MHz,  $\text{CDCl}_3$ ) (ppm): 171.5, 66.7, 54.3, 53.6, 37.2, 35.4, 30.5. Anal. Calcd for  $\text{C}_9\text{H}_{18}\text{N}_2\text{O}_2$ : Found: C, 58.04; H, 9.74; N, 15.04; O, 17.18. C, 57.99; H, 9.85; N, 14.93; O, 17.23.

3-(4-Ethylpiperazin-1-yl)-*N,N*-dimethylpropanamide (Table 2, entry 8)

$^1\text{H}$  NMR (400 MHz,  $\text{CDCl}_3$ ) (ppm): 5.04(s, 2H), 2.91(s, 3H), 2.82(s, 3H), 2.63-2.67(m, 2H), 2.49(s, 4H), 2.44(d, 4H,  $J=8.4\text{Hz}$ ), 2.37(d, 2H,  $J=7.2\text{Hz}$ ), 0.99(t, 3H,  $J=7.2\text{Hz}$ );  $^{13}\text{C}$  NMR (100 MHz,  $\text{CDCl}_3$ ) (ppm): 171.4, 72.5, 61.3, 53.6, 52.4, 52.0, 51.9, 37.1, 35.3, 30.5, 11.4. Anal. Calcd for  $\text{C}_{11}\text{H}_{23}\text{N}_3\text{O}$ : C, 61.93; H, 10.87; N, 19.70; O, 7.50. Found: C, 61.86; H, 10.95; N, 19.64; O, 7.55.

*N*-isopropyl-3-morpholinopropanamide (Table 2, entry 9)

$^1\text{H}$  NMR (400 MHz,  $\text{CDCl}_3$ ) (ppm): 7.95(s, 1H), 3.99-4.08(m, 1H), 3.73(d, 4H,  $J=3.6\text{Hz}$ ), 2.62(t, 2H,  $J=6.4\text{Hz}$ ), 2.51(s, 4H), 2.35(t, 2H,  $J=6.4\text{Hz}$ ), 1.16(t, 3H,  $J=2.4\text{Hz}$ ), 1.14(t, 3H,  $J=2.4\text{Hz}$ );  $^{13}\text{C}$  NMR (100 MHz,  $\text{CDCl}_3$ ) (ppm): 171.2, 67.0, 54.4, 52.9, 40.8, 32.0, 22.9. Anal. Calcd for  $\text{C}_{10}\text{H}_{20}\text{N}_2\text{O}_2$ : C, 59.97; H, 10.07; N, 13.99; O, 15.98. Found: C, 59.86; H, 10.20; N, 13.89; O, 16.05.

*N*-isopropyl-3-(pyrrolidin-1-yl)propanamide (Table 2, entry 10)

$^1\text{H}$  NMR (400 MHz,  $\text{CDCl}_3$ ) (ppm): 8.10(s, 1H), 3.95-4.04(m, 1H), 2.76(t, 2H,  $J=6.4\text{Hz}$ ), 2.59(s, 4H), 2.37(t, 3H,  $J=6.4\text{Hz}$ ), 1.78-1.81(m, 4H), 1.10(d, 6H,  $J=6.4\text{Hz}$ );  $^{13}\text{C}$  NMR (100 MHz,  $\text{CDCl}_3$ ) (ppm): 171.4, 53.2, 51.6, 40.7, 34.2, 23.5, 22.7. Anal. Calcd for  $\text{C}_{10}\text{H}_{20}\text{N}_2\text{O}$ : C, 65.18; H, 10.94; N, 15.20; O, 8.68. Found: C, 65.14; H, 10.99; N, 15.16; O, 8.71.

*N*-(*tert*-butyl)-3-(4-methylpiperidin-1-yl)propanamide (Table 2, entry 12)

$^1\text{H}$  NMR (400 MHz,  $\text{CDCl}_3$ ) (ppm): 8.59(s, 1H), 2.91(d, 2H,  $J=11.6\text{Hz}$ ), 2.55(t, 2H,  $J=6.0\text{Hz}$ ), 2.27(t, 2H,  $J=6.0\text{Hz}$ ), 2.18(s, 1H), 1.94-2.00(m, 2H), 1.69(d, 2H,  $J=12.8\text{Hz}$ ), 1.34(s, 9H), 1.12-1.22(m, 2H), 0.94(d, 3H,  $J=6.4\text{Hz}$ );  $^{13}\text{C}$  NMR (100 MHz,  $\text{CDCl}_3$ ) (ppm): 172.0, 54.4, 53.1, 50.3, 34.5, 33.2, 30.7, 28.9, 21.8. Anal. Calcd for  $\text{C}_{13}\text{H}_{26}\text{N}_2\text{O}$ : C, 68.98; H, 11.58; N, 12.38; O, 7.06. Found: C, 68.93; H, 11.63; N, 12.35; O, 7.09

*N*-(hydroxymethyl)-3-(4-ethylpiperazin-1-yl)propanamide (Table 2, entry 13)

$^1\text{H}$  NMR (400 MHz,  $\text{CDCl}_3$ ) (ppm): 8.83(s, 1H), 4.68(d, 2H,  $J=6.4\text{Hz}$ ), 4.58(s, 2H), 3.57-3.69(m, 1H), 2.63(d, 3H,  $J=6.4\text{Hz}$ ), 2.52(s, 5H), 2.37-2.43(m, 4H), 1.06(t, 3H,  $J=7.2\text{Hz}$ );  $^{13}\text{C}$  NMR (100 MHz,  $\text{CDCl}_3$ ) (ppm): 173.9, 63.8, 53.5, 52.5, 52.4, 52.2, 52.1, 52.0, 32.3, 11.6. Anal. Calcd for  $\text{C}_{10}\text{H}_{21}\text{N}_3\text{O}_2$ : C, 55.79; H, 9.83; N, 19.52; O, 14.86. Found: C, 55.63; H, 10.02; N, 19.40; O, 14.95.

*N*-(hydroxymethyl)-3-(4-methylpiperidin-1-yl)propanamide (Table 2, entry 14)

$^1\text{H}$  NMR (400 MHz,  $\text{CDCl}_3$ ) (ppm): 8.98(s, 1H), 4.69(d, 1H,  $J=6.0\text{Hz}$ ), 3.70(d, 1H,  $J=3.2\text{Hz}$ ), 3.58(d, 1H,  $J=3.2\text{Hz}$ ), 3.09(d, 2H,  $J=11.6\text{Hz}$ ), 2.82(s, 2H), 2.52(s, 2H), 2.19-2.24(m, 2H), 1.96(s, 1H), 1.68(d, 2H,  $J=13.2\text{Hz}$ ), 1.44(s, 1H), 1.30-1.43(m, 2H), 0.92(q, 3H,  $J=6.4\text{Hz}$ );  $^{13}\text{C}$  NMR (100 MHz,  $\text{CDCl}_3$ ) (ppm): 173.2, 72.4, 63.7, 61.4, 53.4, 53.0, 33.3, 32.9, 31.9, 29.9, 21.4. Anal. Calcd for  $\text{C}_{10}\text{H}_{20}\text{N}_2\text{O}_2$ : C, 59.97; H, 10.07; N, 13.99; O, 15.98. Found: C, 59.88; H, 10.16; N, 13.93; O, 16.03.

3-(4-Ethylpiperazin-1-yl)-*N*-(2-methyl-4-oxopentan-2-yl)propanamide (Table 2, entry 16)

$^1\text{H}$  NMR (400 MHz,  $\text{CDCl}_3$ ) (ppm): 8.57(s, 1H), 3.68(t, 1H,  $J=4.4\text{Hz}$ ), 3.55(t, 1H,  $J=4.4\text{Hz}$ ), 2.96(s, 2H), 2.65-2.75(m, 2H), 2.53(t, 4H,  $J=6.0\text{Hz}$ ), 2.37-2.43(m, 4H), 2.14(t, 2H,  $J=6.0\text{Hz}$ ), 2.04(s, 3H), 1.31(s, 6H), 1.05(t, 3H,  $J=7.2\text{Hz}$ );  $^{13}\text{C}$  NMR (100 MHz,  $\text{CDCl}_3$ ) (ppm): 207.6, 172.0,

72.5, 61.4, 53.7, 52.7, 52.2, 52.0, 51.2, 50.5, 32.7, 31.5, 27.8, 11.8. Anal. Calcd for C<sub>15</sub>H<sub>29</sub>N<sub>3</sub>O<sub>2</sub>: C, 63.57; H, 10.31; N, 14.83; O, 11.29. Found: C, 63.52; H, 10.37; N, 14.79; O, 11.32.

*N*-(2-methyl-4-oxopentan-2-yl)-3-morpholinopropanamide (Table 2, entry 17)

<sup>1</sup>H NMR (400 MHz, CDCl<sub>3</sub>) (ppm): 8.42(s, 1H), 3.74(t, 4H, *J*=4.8Hz), 3.00(s, 2H), 2.58(t, 2H, *J*=6.0Hz), 2.53(s, 4H), 2.26(t, 2H, *J*=6.0Hz), 2.08(s, 3H), 1.36(s, 6H); <sup>13</sup>C NMR (100 MHz, CDCl<sub>3</sub>) (ppm): 207.5, 171.8, 66.9, 54.3, 52.7, 51.2, 50.4, 32.5, 31.5, 27.8. Anal. Calcd for C<sub>13</sub>H<sub>24</sub>N<sub>2</sub>O<sub>3</sub>: C, 60.91; H, 9.44; N, 10.93; O, 18.72. Found: C, 60.79; H, 9.57; N, 10.86; O, 18.78.

3-(4-(2-Hydroxyethyl)piperazin-1-yl)-1-morpholinopropan-1-one (Scheme 2)

<sup>1</sup>H NMR (400 MHz, CDCl<sub>3</sub>) (ppm): 3.69-3.71(m, 1H), 3.61-3.68(m, 4H), 3.60(s, 1H), 3.55-3.58(m, 3H), 3.44(t, 4H, *J*=4.4Hz), 2.68-2.72(m, 2H), 2.51-2.54(t, 8H, *J*=4.4Hz), 2.49(t, 2H, *J*=4.4Hz); <sup>13</sup>C NMR (100 MHz, CDCl<sub>3</sub>) (ppm): 170.3, 72.4, 66.8, 66.6, 61.5, 59.5, 57.8, 53.8, 53.0, 52.7, 45.9, 41.9, 30.5. Anal. Calcd for C<sub>13</sub>H<sub>25</sub>N<sub>3</sub>O<sub>3</sub>: C, 57.54; H, 9.29; N, 15.49; O, 17.69. Found: C, 57.41; H, 9.42; N, 15.41; O, 17.76.

## Acknowledgements

We are grateful for the financial supports for this research by the National Natural Science Foundation of China (Grant 21106090 and 21176170), Foundation of Low Carbon Fatty Amine Engineering Research Center of Zhejiang Province (2012E10033), and Zhejiang Provincial Natural Science Foundation of China (No. LY12B02004).

## References

[1] (a) You, L.; Feng, S.; An, R.; Wang, X.; Bai, D. *Tetrahedron Lett.* **2008**, *49*, 5147. (b) Sendzik,

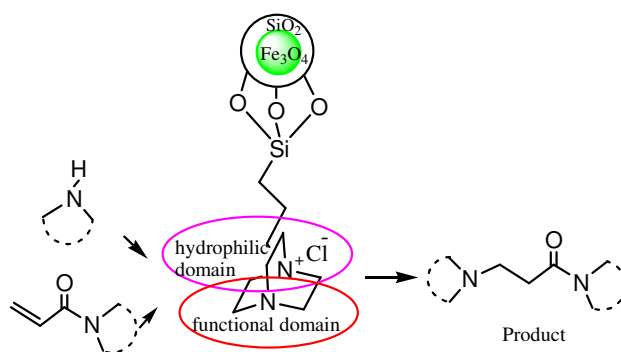
- M.; Janc, J. W.; Cabuslay, R.; Honigberg, L.; Mackman, R. L.; Magill, C.; Squires, N.; Waldeck, N. *Bioorg. Med. Chem. Lett.* **2004**, *14*, 3181. (c) Kitagawa, K.; Mizobuchi, N.; Hama, T.; Hibi, T.; Konishi, R.; Futaki, S. *Chem. Phar. Bull.* **1997**, *45*, 1782. (d) Adessi, C.; Frossard, M. J.; Boissard, C.; Fraga, S.; Bieler, S.; Ruckle, T.; Vilbois, F.; Robinson, S. M.; Mutter, M.; Banks, W. A.; Soto, C. *J. Biol. Chem.* **2003**, *278*, 13911. (e) Kowalchick, J. E.; Leiting, B.; Pryor, K. D.; Marsilio, F.; Wu, J. K.; He, H.; Lyons, K. A.; Eiermann, G. J.; Petrov, A.; Scapin, G.; Patel, R. A.; Thornberry, N. A.; Weber, A. E.; Kim, D. *Bioorg. Med. Chem. Lett.* **2007**, *17*, 5934. (f) Harrison, C. L.; Krawiec, M.; Forslund, R. E.; Nugent, W. A. *Tetrahedron* **2011**, *67*, 41.
- [2] Ibach, B.; Haen, E. *Curr. Pharm. Des.* **2004**, *10*, 231.
- [3] Semple, J. E.; Owens, T. D.; Nguyen, K.; Levy, O. E. *Org. Lett.* **2000**, *2*, 2769.
- [4] (a) Kim, H. J.; Kwak, W. Y.; Min, J. P.; Sung, S. Y.; Kim, H. D.; Kim, M. K.; Kim, H. S.; Park, K. J.; Son, M. H.; Kim, S. H.; Lee, B. J. *Bioorg. Med. Chem. Lett.* **2012**, *22*, 5545. (b) Chhiba, V.; Bode, M. L.; Mathiba, K.; Kwezi, W.; Brady, D. *J. Mol. Catal. B: Enzym.* **2012**, *76*, 68. (c) Heck, T.; Seebach D.; Osswald, S.; ter Wiel, M. K. J.; Kohler, H. P. E.; Geueke, B. *ChemBioChem* **2009**, *10*, 1558. (d) Biaggi, C.; Benaglia, M.; Puglisi, A. *J. Organometal. Chem.* **2007**, *692*, 5795.
- [5] (a) Chaudhuri, M. K.; Hussain, S.; Kantam, M. L.; Neelima, B. *Tetrahedron Lett.* **2005**, *46*, 8329. (b) Khan, A. T.; Parvin, T.; Gazi, S.; Choudhury, L. H. *Tetrahedron Lett.* **2007**, *48*, 3805. (c) Yang, L.; Xu, L.-W.; Xia, C.-G. *Tetrahedron Lett.* **2005**, *46*, 3279. (d) Azizi, N.; Saidi, M. R. *Tetrahedron* **2004**, *60*, 383. (e) Kantam, M. L.; Neeraja, V.; Kavita, B.; Neelima, B.; Chaudhuri, M. K.; Hussain, S. *Adv. Synth. Catal.* **2005**, *347*, 763. (f) Alleti, R.; Oh, W. S.; Perambuduru,

- M.; Ramana, C. V.; Reddy, V. P. *Tetrahedron Lett.* **2008**, *49*, 3466. (g) Nath, J.; Chaudhuri, M. K. *Catal. Lett.* **2009**, *133*, 388. (h) Ying, A.-G.; Liu, L.; Wu, G.-F.; Chen, G.; Chen, X.-Z.; Ye, W.-D. *Tetrahedron Lett.* **2009**, *50*, 1653. (i) Ying, A.; Zheng, M.; Xu, H.; Qiu, F.; Ge, C. *Res. Chem. Intermed.* **2011**, *37*, 883. (j) You, L.; Feng, S.; An, R.; Wang, X.; Bai, D. *Tetrahedron Lett.* **2008**, *49*, 5147.
- [6] Badu-Tawiah, A. K.; Campbell, D. I.; Cooks, R. G. *J. Am. Soc. Mass. Spectrom.* **2012**, *23*, 1461.
- [7] See recently published reviews: (a) Lu, A. H.; Salabas, E. L.; Schüth, F. *Angew. Chem. Int. Ed.* **2007**, *46*, 1222. (b) Gawande, M. B.; Branco, P. S.; Varma, R. S. *Chem. Soc. Rev.* **2013**, *42*, 3371. (c) Nasir Baig, R. B.; Varma, R. S. *Chem. Commun.* **2013**, *49*, 752.
- [8] (a) Du, Q.; Zhang, W.; Ma, H.; Zheng, J.; Zhou, B.; Li, Y. *Tetrahedron* **2012**, *68*, 3577. (b) Lee, J.; Chung, J.; Byun, S. M.; Kim, B. M.; Lee, C. *Tetrahedron* **2013**, *69*, 5660. (c) Jin, X.; Zhang, K.; Sun, J.; Wang, J.; Dong, Z.; Li, R. *Catal. Commun.* **2012**, *26*, 199. (d) Gawande, M. B.; Rathi, A. K.; Nogueira, I. D.; Varma, R. S.; Branco, P. S. *Green Chem.* **2013**, *15*, 1895. (e) Atashkar, B.; Rostami, A.; Tahmasbi, B. *Catal. Sci. Technol.* **2013**, *3*, 2140. (f) Sheykhan, M.; Ma'mani, L.; Ebrahimi, A.; Heydari, A. *J. Mol. Catal. A: Chem.* **2011**, *335*, 253. (g) Xu, H.-J.; Wan, X.; Shen, Y.-Y.; Xu, S.; Feng, Y.-S. *Org. Lett.* **2012**, *14*, 1210. (h) Hu, A.; Yee, G. T.; Lin, W. *J. Am. Chem. Soc.* **2005**, *127*, 12486. (i) Hu, H.; Liu, S.; Lin, W. *RSC Adv.* **2012**, *2*, 2576. (j) Riente, P.; Mendoza, C.; Pericás, M. A. *J. Mater. Chem.* **2011**, *21*, 7350.
- [9] (a) Brozinski, H. L.; Delaney, J. P.; Henderson, L. C. *Aust. J. Chem.* **2013**, *66*, 844. (b) Lombardo, M.; Trombini, C. *ChemCatChem* **2010**, *2*, 135. (c) Khan, S. S.; Shah, J.; Liebscher, J. *Tetrahedron* **2011**, *67*, 1812. (d) Jin, X.; Yang, D.; Xu, X.; Yang, Z. *Chem. Commun.* **2012**,

- 48, 9017. (e) dos Santos, M. R.; Gomes, A. F.; Gozzo, F. C.; Suarez, P. A.; Neto, B. A. D. *ChemSusChem*. **2012**, *5*, 2383.
- [10] Zhang, Q.; Su, H.; Luo, J.; Wei, Y. *Green Chem.* **2012**, *14*, 201.
- [11] Kong, Y.; Tan, R.; Zhao, L.; Yin, D. *Green Chem.* **2013**, *15*, 2422.
- [12] (a) Nishio, K.; Ikeda, M.; Gokob, N.; Tsubouchi, S.; Narimatsua, H.; Mochizuki, Y.; Sakamoto, S.; Sandhuc, A.; Abe, M.; Handa, H. *J. Magn. Magn. Mater.* **2007**, *310*, 2408. (b) Y. Jiang, C. Guo, H. Gao, H. Xia, I. Mahmood, C. Liu, H. Liu, *AIChE J.* **2012**, *58*, 1203.
- [13] Deng, Y. H.; Qi, D. W.; Deng, C. H.; Zhang, X. M.; Zhao, D. Y. *J. Am. Chem. Soc.* **2008**, *130*, 28.
- [14] Jiang, Y.; Jiang, J.; Gao, Q.; Ruan, M.; Yu, H.; Qi, L. *Nanotechnology* **2008**, *19*, 75714.
- [15] Lee, J.; Lee, Y.; Youn, J. K.; Na, H. B.; Yu, T.; Kim, H.; Lee, S. M.; Koo, Y. M.; Kwak, J. H.; Park, H. G.; Chang, H. N.; Hwang, M.; Park, J. G.; Kim, J.; Hyeon, T. *Small* **2008**, *4*, 143.
- [16] Yang, H.; Li, S.; Wang, X.; Zhang, F.; Zhong, X.; Dong, Z.; Ma, J. *J. Mol. Catal. A: Chem.* **2012**, *363*, 404.
- [17] Wang, G.; Yu, N.; Peng, L.; Tan, R.; Zhao, H.; Yin, D.; Qiu, H.; Fu, Z.; Yin, D. *Catal. Lett.* **2008**, *123*, 252.
- [18] (a) Marcoux, D.; Bindschadler, P.; Speed, A. W. H.; Chiu, A.; Pero, J. E.; Borg, G. A.; Evans, D. A. *Org. Lett.* **2011**, *13*, 3758. (b) Verma, S.; Mungse, H. P.; Kumar, N.; Choudhary, S.; Jain, S. L.; Sain, B.; Khatri, O. P. *Green Chem.* **2011**, *47*, 12673. (c) Goldfarb, D. S. US 20090163545 A1, **2009**.

Ionic tagged DABCO grafted on magnetic nanoparticles: a water-compatible catalyst for aqueous aza-Michael addition of amines to  $\alpha,\beta$ -unsaturated amides

Anguo Ying<sup>a\*</sup>, Shuo Liu<sup>b</sup>, Yuxiang Ni<sup>b</sup>, Fangli Qiu<sup>a</sup>, Songlin Xu<sup>b\*</sup>, Wenyuan Tang<sup>a</sup>



A water compatible DABCO grafted on magnetic nanoparticles with ionic tag has been developed and used to catalyze the aza-Michael addition.

\* Corresponding authors. Tel/fax: +86 576 88660359.

E-mail address: yinganguo@163.com or [agying@tzc.edu.cn](mailto:agying@tzc.edu.cn) (A. Ying), [slxu@tju.edu.cn](mailto:slxu@tju.edu.cn) (S. Xu).

Electronic supplementary information (ESI) available: detailed NMR spectra of IS and unknown addition products.